Density Functional Studies on the Pauson−Khand Reaction

Masahiro Yamanaka and Eiichi Nakamura*

Contribution from the Department of Chemistry, The University of Tokyo, Bunkyo-ku, Tokyo 113-0033, Japan

Received September 1, 2000. Revised Manuscript Received January 5, 2001

Abstract: The Pauson−Khand reaction represents a one-step $Co_2(CO)_8$-catalyzed synthesis of cyclopentenone through [2 + 2 + 1] assembly of one molecule each of alkene, alkyne, and carbon monoxide. Density functional studies (B3LYP/631LAN) on the reaction pathway of the Pauson−Khand (PK) reaction reported here for the first time provides valuable information on the structures and energetics of various intermediates and transition states. The PK reaction consists of olefin insertion, CO insertion, and reductive elimination steps. The olefin insertion step was found to be an irreversible step that determines the stereo- and regiochemistry of the overall reaction. The following steps are low activation energy processes and reversible. The bond-forming events occur only on one of the two metal atoms, while the second metal atom not only acts as an anchor that fixes the metal cluster to the organic substrate but also exerts electronic influences on the reaction at the first atom.

Reported first in 1973,[1] the Pauson−Khand (PK) reaction is receiving increasing attention from synthetic chemists in recent years.[2] The reaction represents a one-step $Co_2(CO)_8$-catalyzed synthesis of the cyclopentenone ring system through [2 + 2 + 1] assembly of one molecule each of alkene, alkyne, and carbon monoxide (eq 1).

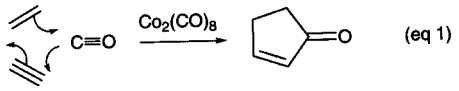

(eq 1)

Despite the great utility of the reaction, there has been a paucity of mechanistic information as was pointed out in a recent review.[1] Although the pathway suggested by Magnus in 1985[3] has been successfully employed as a working model for synthetic chemists (Scheme 1), it has never been subjected to detailed mechanistic studies. The Magnus mechanism involves reversible ligand exchange of a CO molecule and an alkene on a Co_2/alkyne complex followed by carbon−carbon bond formation at the less hindered end of the alkyne and the alkene to form a metallocycle. CO insertion and reductive elimination afford the cyclopentenone/Co complex. In recent modifications,[1,4,5] the final product liberates the cyclopentenone, and the cobalt moiety becomes engaged in further cycles to make the overall reaction catalytic with respect to the cobalt catalyst.

Scheme 1. Magnus Pathway of the PK Reaction

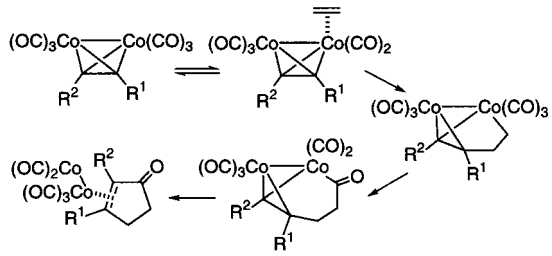

The lack of experimental mechanistic information is due to the fact that once the Co_2/acetylene complex (detected experimentally)[6] is formed in the reaction mixture, it goes immediately to the product without any trace of observable intermediates. Experimental information on the C−C bond-forming steps has therefore been scarce. Pursuing our long-standing interest in the chemistry of polymetallic organometallic clusters,[7] we carried out quantum mechanical studies on the Magnus pathway of the PK reaction, which provided the first set of information on the structures of intermediates and transition states (TS) as well as on the energetics of the reaction.

Computational Methods

All calculations were performed with a GAUSSIAN 98 package.[8] The density functional theory (B3LYP) method[9] was employed. The method is now known to give reliable results in the theoretical analysis of transition metal reactions.[10] Geometries were optimized with the basis sets denoted 631LAN consisting of the LANL2DZ basis set including a double-ζ valence basis set with the Hay and Wadt effective core potential (ECP)[11] for Co and the 6-31G(d) basis set for the rest. For most stationary points (Figure 2, data in parentheses), a single-point

(1) (a) Khand, I. U.; Knox, G. R.; Pauson, P. L.; Watts, W. E.; Foreman, M. I. *J. Chem. Soc., Perkin. Trans. 1* **1973**, 977−981. For recent reviews see: (b) Fletcher, A. J.; Christie, S. D. R. *J. Chem. Soc., Perkin. Trans. 1* **2000**, 1657−1668. (c) Brummond, K. M.; Kent, J. L. *Tetrahedron* **2000**, *56*, 3263−3283. (d) Geis, O.; Schmalz, H. G. *Angew. Chem., Int. Ed.* **1998**, *37*, 911−914. (e) Schore, N. E. In Comprehensive *Organometallic Chemistry II*, Hegedus, L. S., Ed.; Pergamon: Oxford, 1995; Vol. 12, pp 703−739. (f) Schore, N. E. *Org. React.* **1991**, *40*, 1−90. (g) For earlier semiempirical molecular orbital and molecular mechanics studies for explanation of stereoselectivity, see: Verdaguer, X.; Vázquez, J.; Fuster, G.; Bernardes-Génisson, V.; Greene, A. E.; Moyano, A.; Pericas, M. A.; Riera, A. *J. Org. Chem.* **1998**, *63*, 7037−7052. Breczinski, P. M.; Stumpf, A.; Hope, H.; Krafft, M. E.; Casalnuovo, J. A.; Schore, N. E. *Tetrahedron* **1999**, *55*, 6797−6812.

(2) For instance, a key word search in *Chem. Abstr*. indicated over 240 publications after 1990, of which over 70 papers appeared after 1999.

(3) Magnus, P.; Priciple, L. M. *Tetrahedron Lett.* **1985**, *26*, 4851−4854.

(4) Hayashi, M.; Hashimoto, Y.; Yamamoto, Y.; Usuki, J.; Saigo, K. *Angew. Chem., Int. Ed.* **2000**, *39*, 631−633.

(5) Pagenkopf, B. L.; Livinghouse, T. *J. Am. Chem. Soc.* **1996**, *118*, 2285−2286.

(6) Dickson, R. S.; Fraser, P. J. *Adv. Organomet. Chem.* **1974**, *12*, 323.

(7) Cf. Nakamura, M.; Nakamura, E.; Koga, N.; Morokuma, K. *J. Am. Chem. Soc.* **1993**, *115*, 11016−11017. Nakamura, E.; Mori, S.; Nakamura, M.; Morokuma, K. *J. Am. Chem. Soc.* **1997**, *119*, 4887−4899. Nakamura, E.; Hirai, A.; Nakamura, M. *J. Am. Chem. Soc.* **1999**, *121*, 8665−8666. Nakamura, E.; Yamanaka, M.; Mori, S. *J. Am. Chem. Soc.* **2000**, *122*, 1826−1827. Nakamura, E.; Mori, S. *Angew. Chem., Int. Engl.* **2000**, *39*, 3751−3771.

10.1021/ja005565+ CCC: $20.00
Published on Web 01/31/2001

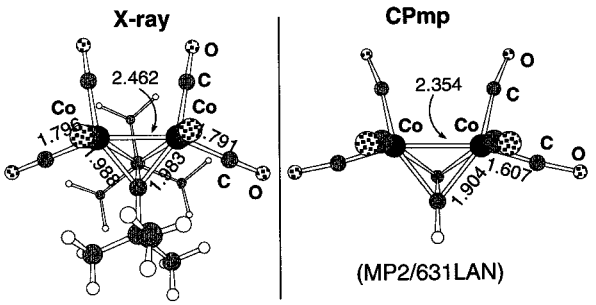

Figure 1. Co_2/acetylene complex structure determined by X-ray crystallography for a 2,2,5,5-tetramethyl-3-hexyne complex and the MP2/631LAN-optimized structure of an acetylene complex.

energy calculation for the B3LYP/631LAN-optimized geometry was also performed with the better basis sets, 6311SDD consisting of Stuttgart ECP[12] for Co and the 6-311+G(d) for the rest. As shown in Figure 2, the energetics obtained with this basis set was qualitatively the same as that obtained with the 631LAN basis set. The structure of **CP1** calculated by the B3LYP/631LAN method (Figure 2, **CP1**) is very close to the structures of Co_2/alkyne complexes determined by X-ray crystallography (cf. Figure 1).[13] The MP2/631LAN-optimized geometry (Figure 1, **CPmp**) is also similar to that of X-ray crystallography structures, while the Co−Co and Co−CO bonds of the MP2 structure are ca. 0.1 Å shorter than those of X-ray structures. The Co−acetylene bonds are also much shorter in the MP2 structure than in the B3LYP or X-ray structure. It has been shown by the intrinsic reaction coordinate (IRC) analysis[14] followed by the geometry optimization that the sequence of the coordinatively saturated stationary points **CP3**-**TS1**-**CP4**, **CP5**-**TS2ab**-**CP6ab**, and **CP7ab**-**TS3ab** are smoothly connected along the reaction coordinate. Stability analyses[15] have been performed to determine if the Kohn−Sham (KS) solutions are stable with respect to variations which break spin- and spatial symmetry. Although very small external instability was found in the restricted KS solutions for some stationary points, we confirmed that such instability does not affect the reported RB3LYP/631LAN results through comparison of the geometries, total energies, and molecular orbitals obtained under restricted and unrestricted conditions.

The Boys localization procedure was performed to obtain localized Kohn−Sham orbitals (LOs)[16] from the occupied B3LYP/631LAN level Kohn−Sham molecular orbitals for the B3LYP/631LAN geometries. Natural charges were calculated by the natural population analysis at the same level as the one used for geometry optimization.[17]

Scheme 2. Bimetallic Pathway of the PK Reaction

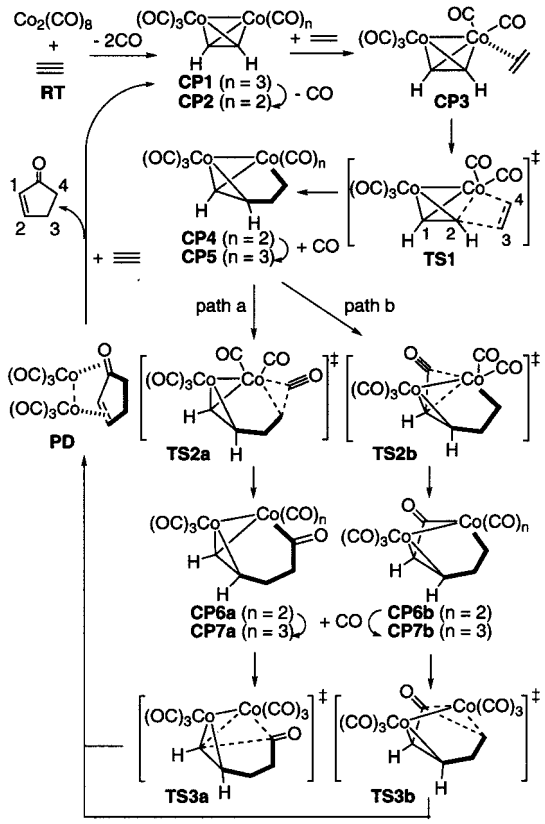

Results and Discussion

Reaction Pathway of PK Reaction. In Scheme 2 and Figure 2 are shown the reaction course and the energy profile that we probed for the $Co_2(CO)_8$-mediated PK reaction (energies and geometries at B3LYP/631LAN unless otherwise noted). As is known experimentally,[6] the first reaction of acetylene with $Co_2(CO)_8$ is the formation of a Co_2/acetylene complex **CP1** with loss of gaseous CO (10.0 kcal/mol endothermic). Ligand exchange between CO (good σ donor and π acceptor) and ethylene (poor π acceptor) on **CP1** via a coordinatively unsaturated complex **CP2** produces a themodynamically unfavorable ethylene complex **CP3**. **CP3** smoothly goes to Co−metallocycle **CP4** via **TS1**-the first C−C bond formation step. The activation energy of this step is 14.4 kcal/mol (B3LYP/6311SDD//B3LYP/631LAN: 14.6 kcal/mol). Exothermic take-up of CO by **CP4** gives **CP5**. Although it has been silently assumed in the conventional scheme[3] that the migratory insertion of CO occurs only at the CH_2 carbon (path a), an alternative path (path b; insertion of the alkenyl carbon) does exist. It was, however, found to be higher in energy than path a. Thus, the reaction will proceed through **TS2a** with preferential migratory insertion of CO on the CH_2 side with an activation barrier of 8.7 kcal/mol (B3LYP/6311SDD//B3LYP/631LAN: 10.0 kcal/mol). The alternative pathway via **TS2b** requires an activation barrier of 12.9 kcal/mol (B3LYP/6311SDD//B3LYP/631LAN: 14.4 kcal/mol). Subsequent CO coordination (**CP6a** to **CP7a**) followed by reductive elimination (**TS3a**) gives the product **PD**. The activation energy for **TS3a** is 3.5 kcal/mol (B3LYP/6311SDD//B3LYP/631LAN: 4.1 kcal/mol). The alternative pathway via **TS3b** also requires a much larger activation energy barrier of 14.7 kcal/mol (B3LYP/6311SDD//B3LYP/631LAN: 16.1 kcal/mol) than path a. Ligand exchange between cyclo-

(8) Frisch, M. J.; Trucks, G. W.; Schlegel, H. B.; Scuseria, G. E.; Robb, M. A.; Cheeseman, J. R.; Zakrzewski, V. G.; Montgomery, J. A., Jr.; Stratmann, R. E.; Burant, J. C.; Dapprich, S.; Millam, J. M.; Daniels, A. D.; Kudin, K. N.; Strain, M. C.; Farkas, O.; Tomasi, J.; Barone, V.; Cossi, M.; Cammi, R.; Mennucci, B.; Pomelli, C.; Adamo, C.; Clifford, S.; Ochterski, J.; Petersson, G. A.; Ayala, P. Y.; Cui, Q.; Morokuma, K.; Malick, D. K.; Rabuck, A. D.; Raghavachari, K.; Foresman, J. B.; Cioslowski, J.; Ortiz, J. V.; Stefanov, B. B.; Liu, G.; Liashenko, A.; Piskorz, P.; Komaromi, I.; Gomperts, R.; Martin, R. L.; Fox, D. J.; Keith, T.; Al-Laham, M. A.; Peng, C. Y.; Nanayakkara, A.; Gonzalez, C.; Challacombe, M.; Gill, P. M. W.; Johnson, B. G.; Chen, W.; Wong, M. W.; Andres, J. L.; Head-Gordon, M.; Replogle, E. S.; Pople, J. A. *Gaussian 98*, revision A.9; Gaussian, Inc.: Pittsburgh, PA, 1998.

(9) (a) Becke, A. D. *J. Chem. Phys.* **1993**, *98*, 5648−5652. (b) Lee, C.; Yang, W.; Parr, R. G. *Phys. Rev. B* **1988**, *37*, 785−789.

(10) (a) Niu, S.; Hall, M. B. *Chem. Rev.* **2000**, *100*, 353−405. (b) Koga, N.; Morokuma, K. *Chem. Rev.* **1991**, *91*, 823−842.

(11) Wadt, W. R.; Hay, P. J. *J. Chem. Phys.* **1985**, *82*, 299−310.

(12) Dolg, M.; Wedig, U.; Stoll, H.; Preuss, H. *J. Chem. Phys.* **1987**, *86*, 866−872.

(13) Baert, F.; Guelzim, A.; Poblet, J. M.; Wiest, R.; Demuynck, J.; Benard, M. *Inorg. Chem.* **1986**, *25*, 1830.

(14) (a) Fukui, K. *Acc. Chem. Res.* **1981**, *14*, 363−368. (b) Gonzalez, C.; Schlegel, H. B. *J. Chem. Phys.* **1989**, *90*, 2154−2161. (c) Gonzalez, C.; Schlegel, H. B. *J. Phys. Chem.* **1990**, *94*, 5523−5527.

(15) (a) Seeger, R.; Pople, J. A. *J. Chem. Phys.* **1977**, *66*, 3045−3050. (b) Bauernschmitt, R.; Ahlrichs, R. *J. Chem. Phys.* **1996**, *104*, 9047−9052.

(16) (a) Boys, S. F. *Quantum Theory of Atoms, Molecules, and the Solid State*; Lowdin, P. O., Ed.; Academic Press: New York, 1968; pp 253−262. (b) Haddon, R. C.; Williams, G. R. *J. Chem. Phys. Lett.* **1976**, *42*, 453−455. (c) Kohn, W.; Sham, L. *J. Phys. Rev.* **1965**, *140*, A1133−1138.

(17) Reed, A. E.; Weinstock, R. B.; Weinhold, F. *J. Chem. Phys.* **1985**, *83*, 735−746.

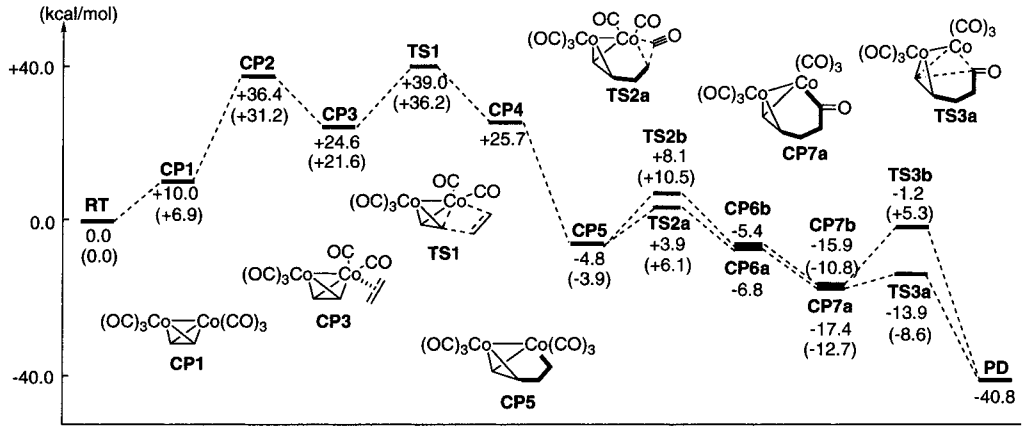

Figure 2. Energetics of the PK reaction at the B3LYP/631LAN level. The values in parentheses are for B3LYP/6311SDD//B3LYP/631LAN.

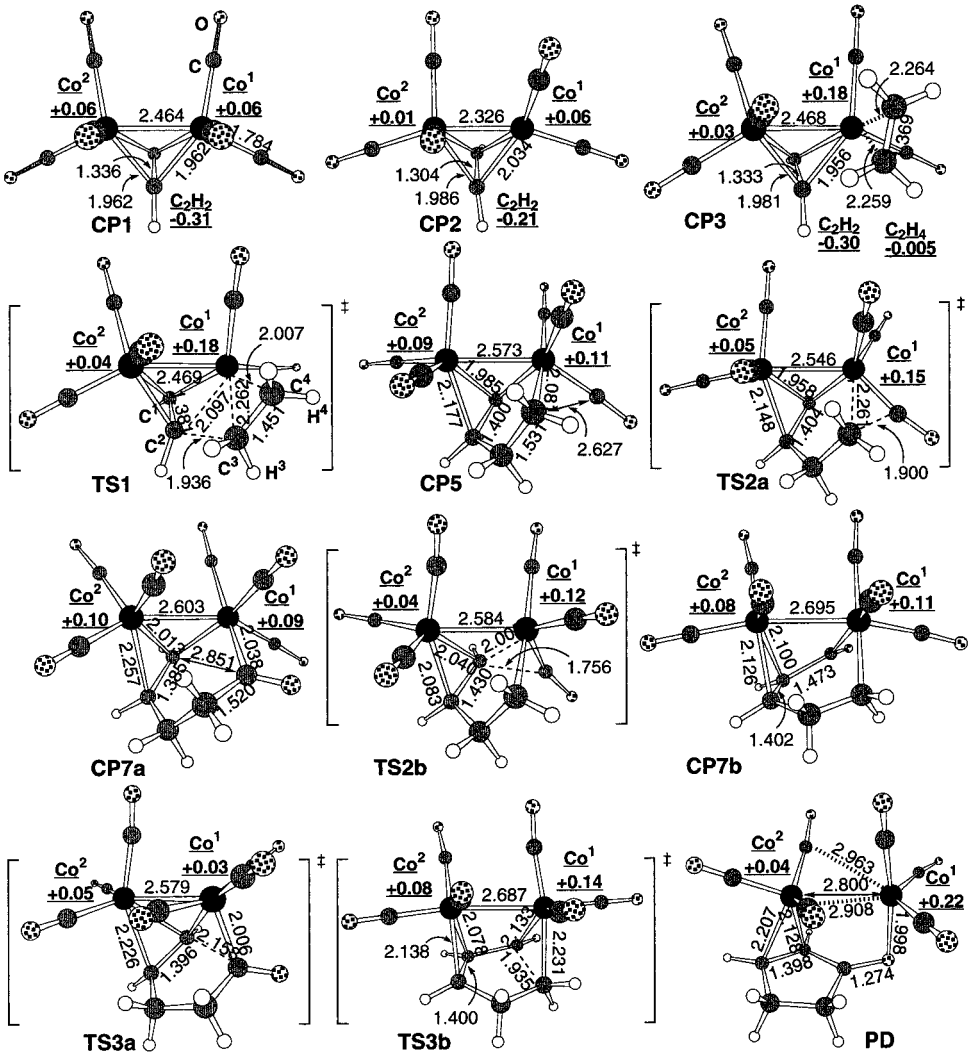

Figure 3. B3LYP/631LAN structures of important stationary points of the PK reaction. Bond lengths are in Å. Natural charges are underlined.

pentenone and acetylene regenerates the starting acetylene complex **CP1**.

As shown in Figure 2, **CP2** and **TS1** represent the two highest energy stationary points, and the **TS1**-to-**CP5** conversion is 43.8 kcal/mol exothermic and irreversible. It is unclear at this time whether the reaction goes through the discrete unsaturated complex **CP2** (26.4 kcal/mol above **CP1**) or through a somewhat lower-energy transition state of an associative CO/ethylene exchange (which we have so far failed to locate). At any event, the following reactions (path a) occur much more easily and are reversible up to **TS1** under the reaction conditions. This energy profile is consistent with the experimental failure to observe any intermediates after **CP1**. The large energy barrier to go to **CP3** by the loss of a CO molecule gives support to the successful use of a weakly coordinating ligand such as $Bu_3P{=}S$[4] or photo irradiation[5] to accelerate the PK reaction.

As is seen in the three-dimensional pictures of the important stationary points (Figure 3), two structural features are noteworthy: the Co−Co bond (2.326−2.695 Å) is retained, and the Co^2 atom remains firmly attached to the acetylene molecule

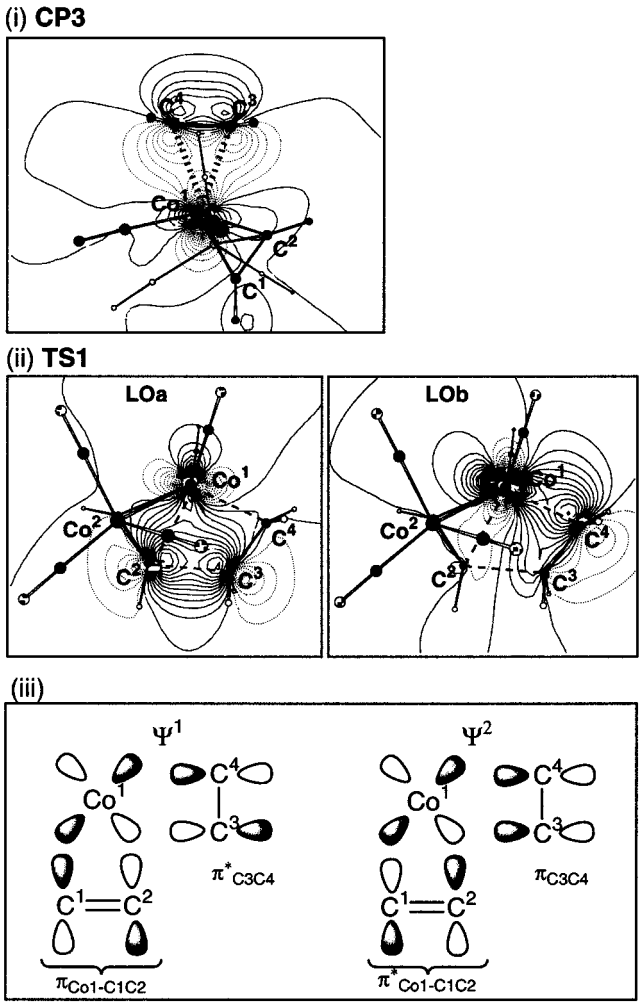

Figure 4. Localized Kohn−Sham orbitals (B3LYP/631LAN) of (i) **CP3** in the $Co^1-C^3-C^4$ plane and (ii) **TS1** in the $Co^1-C^2-C^3$ plane at the contours intervals of 0.025 in e•au^{-3} (iii) schematic orbital interactions (Ψ^1 and Ψ^2).

(Co^2-C^1 or Co^2-C^2 bond lengths of 1.952 to 2.257 Å) throughout the reaction. The acetylene unit in **CP1** has the C−C bond length of 1.336 Å and the C−C−H angle of 142.9° and indicates strong π-back-bonding from the Co d orbital to the acetylene π^* orbital. This is also supported by the large negative natural charge on the acetylene moiety (Co^1, Co^2: +0.06, acetylene: −0.31). While the acetylene unit in **CP3** is also tightly bound to the Co^2 atom (Co^2-C^1, Co^2-C^2, and C^1-C^2 bond lengths of 1.958, 1.981, and 1.333 Å, respectively), the ethylene molecule in **CP3** is rather weakly bound to Co^1 atom as indicated by the nearly planar ethylene geometry (sum of bond angles around $C^3 = 358.0°$, $C^4 = 358.6°$, C^3-C^4 bond length of 1.369 Å and a long distance between ethylene and Co^1). Molecular orbital analysis revealed weak electron donation from ethylene to Co^1 (Figure 4, (i)) and very weak back-donation. The natural charge of the ethylene moiety in **CP3** is almost neutral, and the Co^1 atom has a more positive charge than the Co^2 atom (Co^1: +0.18, Co^2: +0.03).

The TS of olefin insertion (**TS1**) is synthetically the most important step, since the regio- and stereochemistry of bond formation as to (substituted) acetylene, and (substituted) ethylene is determined (discussed later again). In **TS1**, ethylene which was nearly flat in **CP3** is now bent (sum of bond angles around $C^3 = 344.4°$, $C^4 = 349.0°$) and C^3-C^4 bond length of 1.451 Å

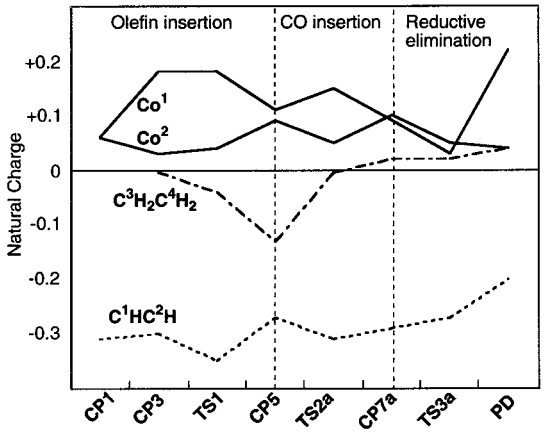

Figure 5. Natural population analysis of Co^1, Co^2, acetylene (C^1HC^2H), and ethylene ($C^3H_2C^4H_2$) for path a.

is elongated by 6.0% from **CP3**. The natural charge of Co atoms in **TS1** is similar to the one in **CP3**.

Boys localized Kohn−Sham orbitals (LOs)[16] of **TS1** (Figure 4, (ii)) illustrates the typical orbital interaction of four-center transition state in olefin insertion.[10] An occupied 3d orbital of Co^1 contributes to the Co^1-C^2 bond by back-donation to acetylene π^* orbital. Orbital interaction between the occupied 3d orbital and the unoccupied acetylene π^* orbital generates the occupied $\pi_{Co1-C1C2}$ orbital and the unoccupied $\pi^*_{Co1-C1C2}$ orbital (Figure 4, (iii)). These orbitals participate in the C^2-C^3 bond formation through interaction with the π- and π^* orbitals of ethylene molecule; namely the occupied $\pi_{Co1-C1C2}$ orbital interacts with the unoccupied ethylene π^* orbital to generate Ψ^1, and the occupied ethylene π orbital interacts with the unoccupied $\pi^*_{Co1-C1C2}$ orbital to generate Ψ^2. LOa and LOb of **TS1** (Figure 4, (ii)) represent a linear combination of these two orbital interactions.

Two isomeric transition structures (**TS2a**: methylene, **TS2b**: alkenyl side) of CO insertion are possible. Two isomeric CO insertion steps and a subsequent CO molecule coordination afford **CP7a** and **CP7b**. While **CP7a** is in a half-chair shape as to the cobaltacyclohexanone moiety, **CP7b** is in a half-boat shape (Figure 3). These geometrical features are reflected in the transition structures **TS2a** and **TS2b**, respectively. The activation energy difference of isomeric CO insertion pathways is caused by these geometrical requirements. The TSs of the reductive elimination (**TS3a** and **TS3b**) include quite complex polycyclic systems, but appear to be remarkably strain free. The Co^2-C^1, Co^2-C^2, and Co^1-Co^2 bonds are slightly elongated. The Co^2 atom acts as an anchor and the bicyclo [2.2.1]structure of the Co_2/acetylene moiety remains stable. The final product **PD** is a dicobalt/enone complex and the ligand exchange between acetylene and enone will regenerate the of dicobalt/acetylene complex **CP1**.

Examination of the natural population[17] for the two cobalt atoms, acethylene (C^1HC^2H), and ethylene ($C^3H_2C^4H_2$) (Figure 5, indicated for path a) revealed an interesting complementary change of the natural charge for the two cobalt atoms. Thus, as the three major events occur on the Co^1 atom, the change of the Co^1 charge is enhanced by the Co^2 atom in the first two events and neutralized in the last. Thus, the Co^2 atom is not a silent spectator but serves as an electron reservoir for the Co^1 atom. The acethylene moiety is negatively charged by back-donation from cobalt atoms and tightly coordinated to the Co^2 atom throughout the reaction. The natural charge of the ethylene moiety goes to the negative side at the first step due to bond formation to the Co^1 atom.

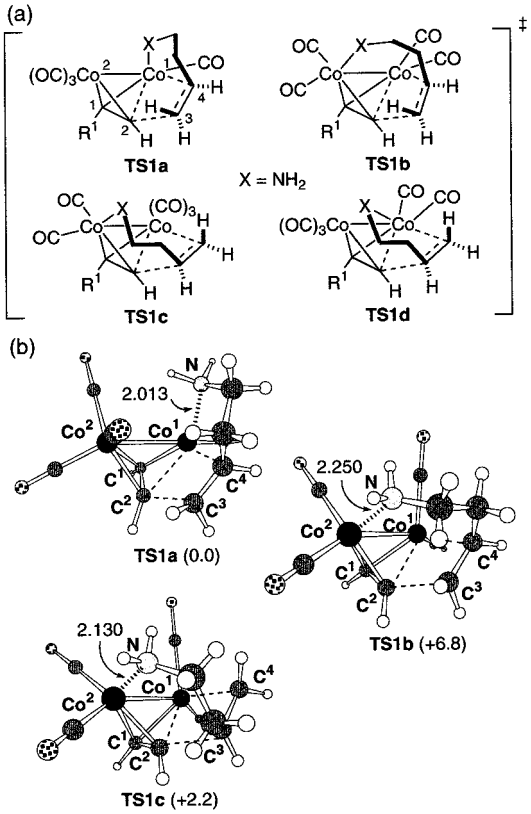

Figure 6. (a) Four possible isomeric TSs of the PK reaction shown in eq 3, (b) B3LYP/631LAN isomeric TSs of the first C−C bond formation in the PK reaction wherein X = NH_2. The geometry of the $Co^1-Co^2-C^1-C^2-C^3-C^4$ skeleton was fixed at that in **TS1** (unsubstituted model), and the remaining part was fully optimized. Distances are in Å. The values in parentheses are relative energies in kcal/mol.

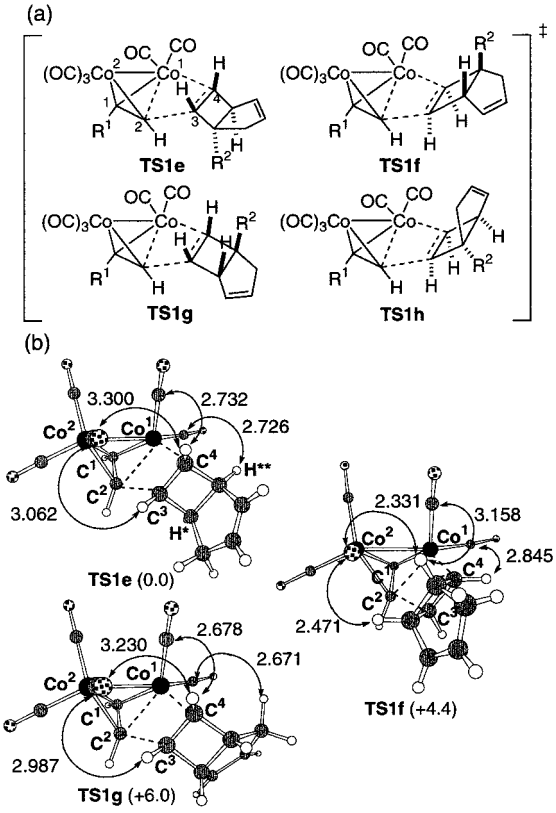

Figure 7. (a) Four possible isomeric TSs of the PK reaction shown in eq 4, (b) B3LYP/631LAN isomeric TSs of the first C−C bond formation in the PK reaction. The geometry of the $Co^1-Co^2-C^1-C^2-C^3-C^4$ skeleton was fixed at that in **TS1** (unsubstituted model), and the remaining part was fully optimized. Distances are in Å. The values in parentheses are relative energies in kcal/mol.

Regio- and Stereoselectivity of PK Reaction. The geometry (Figure 2) and the charge distribution of **TS1** give us clues to understand the experimentally observed selectivity of the PK reaction. First, neither the acetylene nor the ethylene moiety is polarized (C^1H (−0.20), C^2H (−0.15); C^3H_2 (+0.03), C^4H_2 (−0.07)), and therefore, no particularly large electronic effects of substituents on the acetylene or the ethylene molecule are expected in **TS1**. From the geometry of **TS1** (Figure 3) one can see that the C^1 position is less hindered than the C^2 position and will accommodate a subsituent more easily at the C^1 position; such regiochemistry is the one observed in experiments.[1]

As to steric environment around the olefin, both H^3 and H^4 occupied relatively unhindered positions in **TS1** (Figure 3), and we found little difference of steric environment between these two positions in **TS1**. These observations (small steric and electronic effects) are consistent with the lack of regioselectivity for simple 1-alkenes in the PK reaction (eq 2).

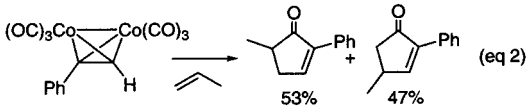

When the olefin possesses a nearby substituent capable of coordinating to a cobalt atom (e.g., Co^1), experiments indicate that such a substituent will be attached to the C^4 atom.[18] Examples of the successful regiocontrol for the PK reaction of an alkene bearing a coordinating heteroatom such as sulfur or nitrogen are shown in eq 3.

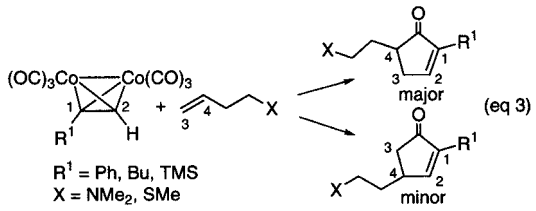

It has been suggested[18] that the heteroatom group is coordinated to one of the metal centers and controls the regioselectivity. One can a priori consider from isomeric **TS**s for the first C−C bond forming step, **TS1a**, **TS1b**, **TS1c**, and **TS1d** (X = NH_2) (Figure 6a). In the interest of time economy, only the geometry of the substituent and the ligand groups was optimized, while the geometry of the core reaction center ($Co^1-Co^2-C^1-C^2-C^3-C^4$) was frozen at the geometry of **TS1** which is the unsubstituted model. Among these TSs, **TS1d** could not be optimized by retaining the internal chelate because the tether unit was too short to maintain such chelation. The relative energies of the three isomeric TSs shown in Figure 6b indicate that **TS1a** is more favored by ca. 2−6 kcal/mol than the other isomeric TSs, which supports the experimental results shown in eq 3. The energetic preference to **TS1a** is largely due to the fact that the directing NH_2 group is more strongly coordinated to the Co^1 atom ($N-Co^1$: 2.013 Å) than those in **TS1b** and **TS1c** ($N-Co^2$: 2.250 Å, $N-Co^2$: 2.131 Å, respectively).

(18) (a) Krafft, M. E. *J. Am. Chem. Soc.* **1988**, *110*, 968−970. (b) Krafft, M. E.; Juliano, C. A. *J. Org. Chem.* **1992**, *57*, 5106−5115.

An experimental example for the diastereofacial selectivity issue is known; namely, only the *exo*-fused product is obtained in the PK reaction of the bicyclo[3.2.0]hept-6-ene shown in eq 4. To probe the diastereofacial selectivity, the relative energies for the TSs **TS1e**, **TS1f**, **TS1g**, and **TS1h** were examined. In this investigation, only the geometry of the substituent and ligand groups was again optimized, while the core skeleton of the reaction center ($Co^1-Co^2-C^1-C^2-C^3-C^4$) was frozen at the geometry of **TS1**. **TS1h** was in an unrealistically high energy in this fixed geometry model. Among three TSs, **TS1e** was found to be overwhelmingly favored over **TS1f** and **TS1g**, which suffer from steric interactions between carbonyl groups and hydrogen atoms (2.33−2.65 Å distances in Figure 7b). Of the two hydrogen atoms marked H* and H** in **TS1e** (Figure 7b), H** suffers from interaction with a neighboring CO ligand (cf. 2.726 Å distance), while H* is strain free. H* must therefore be the hydrogen atom where the R^2 group should be placed in the real system (eq 4). Overall, the fixed geometry modeling

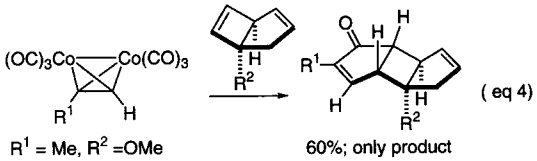

fully supports the experimental results that **TS1e** is the most favored TS. The calculated geometry indicates that the steric effect of CO ligands determines the stereoselectivity of the PK reaction. In the case where a chiral diphosphine molecule[19] (e.g., BINAP) is allowed to coordinate on the cobalt complex bearing a substituted ethylene, such coordination generates diastereoisomerism both in **CP3** and in **TS1** (bearing a substituted ethylene) and hence will produce an enantiomerically enriched subsituted cyclopepentenone product.

In summary, we have explored the reaction pathway of the PK reaction and have shown that the olefin insertion step (**TS1**) is the critical stereo-, and regiochemistry-determining step of the PK reaction. The stages that follow **TS1** are much less synthetically influential. We expect that the geometry of **TS1** and related structures will be useful for the future design of asymmetric PK reactions, the research on which has recently begun.[19] The most important mechanistic finding is that, while the bond-forming events occur only on one metal atom, the other metal atom acts as an anchor and also exerts electronic influences on the other through the metal−metal bond.[20]

Acknowledgment. Generous allotment of computational time from Institute for Molecular Science, Okazaki, Japan, and the Intelligent Modeling Laboratory, The University of Tokyo is gratefully acknowledged.

Supporting Information Available: Geometries of the representative stationary points (PDF). This material is available free of charge via the Internet at http://pubs.acs.org.

JA005565+

(19) Hiroi, K.; Watanabe, T.; Kawagishi, R.; Abe, I. *Tetrahedron Lett.* **2000**, *41*, 891−895. For other asymmetric PK reactions, see refs 1b, c, d, e, and f.

(20) For 3D structures and coordinates, see: http://www.chem.s.u-tokyo.ac.jp/~common/Theo/PK/title.